Hindawi
Mathematical Problems in Engineering
Volume 2022, Article ID 3863267, 11 pages
https://doi.org/10.1155/2022/3863267

Research Article

Gas Seepage Model and Experiment Based on Bedding Effect of Fractured Coal Body

Kunyun Tian[1] **and Erjian Wei**[2]

[1]*School of Resources and Safety Engineering, Henan University of Engineering, Zhengzhou 451191, China*
[2]*School of Resource and Environmental Engineering, Wuhan University of Science and Technology, Wuhan 430081, China*

Correspondence should be addressed to Kunyun Tian; tky1153@163.com and Erjian Wei; weierjian@wust.edu.cn

Received 24 March 2022; Accepted 15 April 2022; Published 9 May 2022

Academic Editor: Conghu LIU

Gas drainage is of great significance for the efficient and safe mining in coal mine, in which the coal seam layer bedding has a great influence on it. For obtaining gas permeability characteristics of coal body with the parallel and vertical bedding in fractured coal under the action of stress loading and unloading, experimental research was carried out employing a three-stress-axis simulation device. Experimental results showed that in the stress loading process, the permeability decreased with increasing effective stress; the decrement was initially rapid albeit it slowed later. With the increase of effective stress, the coal sample underwent three stages, namely, crack compaction, elastic deformation, and plastic deformation. In the stress unloading process, the permeability of coal samples increased with decreasing of effective stress, and the increasing trend of permeability was consistent. The degree of fracture compaction of the parallel bedding coal samples after compression was much higher than that of vertical bedding. In the stress-relieved coal seam, gas drainage boreholes should be arranged vertically to the bedding fissure to maximise the gas drainage effect. A group of parallel and vertical bedding gas drainage holes were arranged in the test mine to investigate the drainage effect. Field engineering application also showed that the drilling direction should be perpendicular to the bedding direction as far as possible, so as to improve the gas drainage effect. The research results can provide a reference for the gas drainage borehole layout, thus maximising the gas extraction efficiency and ensuring the sustainability of mine safety production.

1. Introduction

The bedding is widely distributed in the coal seam and determines its stability, especially the gas flow state [1]. The integrity of a coal body is destroyed by bedding fissures; meanwhile, the stress distribution state changes to a great extent [2], and bedding fissures are one of the main controlling factors that determine the strength of a coal body, its deformation, and gas permeability characteristics. Bedding fissures will develop, penetrate, and deform after mining; this has a great influence on the gas seepage and diffusion, directly determining the characteristics of gas migration and accumulation and then greatly affecting the gas drainage of each coal seam. As is known, gas drainage is the most basic technical measure used to control coal mine gas disasters [3], and coal seam permeability is the most important index used to determine the gas drainage effect [4, 5]. Coal structure is an important index used to determine coal seam permeability. Consequently, gas drainage borehole design, according to the characteristics of different bedding fissures, is essential for improving the gas drainage effect and achieving the best gas drainage.

Research into the influence of coal bedding fissures on permeability has been carried out at home and abroad. Experimental studies of the effect of coal body structure on gas permeability characteristics have been carried out by Huang [6]; research results showed that the effect of coal structure anisotropy on permeability was great and differences in permeability of almost one order of magnitude arose. Research on permeability characteristics of layered natural coal under different loading and unloading has been conducted by Pan et al. [7], and a theoretical model between

fractured coal bedding and the effective stress was established. Using the fluid-solid coupling three-axis servo seepage device with gas coal, a seepage test on two kinds of raw coal samples (parallel and vertical to coal bedding direction) under different stress conditions was carried out by Deng et al. [8]. Results showed that the permeability difference between the two coal samples was mainly caused by the difference of the extent of fracturing in the z-axis direction. Axial effect of multistage loading and unloading on gas seepage in coal body with lower fissure has been conducted by Cen et al. [9], and the results showed that the coal sample goes through three stages of compaction, elastic deformation, and plastic deformation in the process of multistage loading, and the two axial gas permeability decreases with the increase of stress. In the unloading process, the gas permeability in two axial directions was partially recovered. The gas permeability along x-axis of parallel bedding is always greater than that along y-axis of vertical bedding under loading and unloading. A large number of experimental studies on the permeability of coal samples under different bedding conditions have been carried out by Wang et al. [10], Wu et al. [11], and Li et al. [12]; all conclusions showed that coal body bedding affected the permeability characteristics.

All the research results analyse the influence of coal body bedding on gas permeability; these have a certain guiding significance to reasonable gas drainage borehole arrangement. In the actual mining process, a coal body is in a changing stress field [13]. Therefore, it is necessary to examine the gas seepage and failure-deformation characteristics under parallel and vertical bedding directions. For this purpose, large lump coal samples with bedding structures are collected; two different kinds of raw coal samples with parallel and vertical bedding are prepared; and the related research work was carried out in the laboratory. Meanwhile, in order to verify the experimental results, a group of parallel and vertical bedding gas drainage holes were arranged in the test mine to investigate the drainage effect.

2. Experimental Method

2.1. Simulation Experiment System. The independently developed triaxial stress gas permeability simulation experiment device was employed in the experiments, as shown in Figure 1 [14].

2.2. Preparation of Experimental Coal Samples. The coal samples used in this experiment come from the 1,2031 working face in the Xindeng coal mine in Zhengzhou city. The No. 2 coal seam in this coal mine has no obvious geological structural damage in the process of coal forming. This coal seam is a primary structure and is a low-metamorphic rank bituminous coal. The coal seam is mainly horizontally bedded; in addition, the bedding is clearly visible.

The raw samples for the experiment are gained through the following three steps, namely, collection of the large lump coals, coal sample machining in the laboratory, and grinding of the finished product. Collection of the large lump coal underground involved coring with a rock coring drill along the vertical and parallel to the bedding direction. The grinding of the two ends and the sides of the standard cylindrical samples ensured an unevenness of less than 0.02 mm. Finally, the standard coal sample measured Φ 50 mm × 100 mm. The production process of the coal sample was shown in Figure 2.

Two coal samples with parallel bedding were selected, marked as P1 and P2. Meanwhile, the other two coal samples with vertical bedding were selected, marked as V1 and V2. The two types of coal samples are shown in Figure 3.

3. Calculation Method

Initially, the coal body is under a state of static stress (original stress zone). As mining advances, the coal body experiences the process of loading (stress concentration) and unloading (pressure relief belt) [15]. Corresponding to this, the stress loading and unloading path is as follows: under a certain gas pressure (according to the actual situation of the Xindeng coal mine, here, the gas pressure is 0.6 MPa), the axial compression and confining pressure of the coal samples are loaded to 12 MPa; thereafter, confining pressures are unloaded at a uniform rate under constant axial pressure (12 MPa); the rate of confining pressure and axial compression loading and unloading is set to 0.01 MPa/s; and at the same time, the frequency of permeability datum acquisition is set to 5 seconds. Under the same stress loading unloading path, the permeability of parallel and vertical bedding fracture coal samples will be discussed.

Gas flow through the coal samples is collected automatically by the flow meter, and the permeability is calculated from the following formula [16, 17]:

$$k = \frac{2Q_0P_0\mu L}{\left(P_1^2 - P_2^2\right)A}, \tag{1}$$

where k is the coal sample permeability, mD; Q_0 is the seepage rate, cm^3/s; P_0 is the atmospheric pressure at the measuring point, MPa; μ is the gas dynamic viscosity coefficient (10.8×10^{-6} Pa s); P_1 is the inlet gas pressure (0.6 MPa); P_2 is the outlet gas pressure (0.1 MPa); A is the cross-sectional area of coal samples, cm^2; and L is the length of each coal sample, cm. The effective stress of the coal sample is calculated according to the following formula:

$$\sigma_e = \frac{\left(\sigma_z + 2\sigma_w\right)}{3} - \frac{\left(P_1 - P_2\right)}{2}, \tag{2}$$

where σ_e is the effective stress, σ_z is the axial pressure on the coal sample, σ_w is the confining pressure on the coal samples, P_1 is the inlet gas pressure (0.6 MPa), and P_2 is the outlet gas pressure (0.1 MPa). The specific experimental programme is summarised in Table 1.

4. Experimental Results and Analysis

4.1. Experimental Results. Under the action of stress loading and unloading, the permeability of coal samples with the parallel and vertical bedding are listed in Tables 2 and 3.

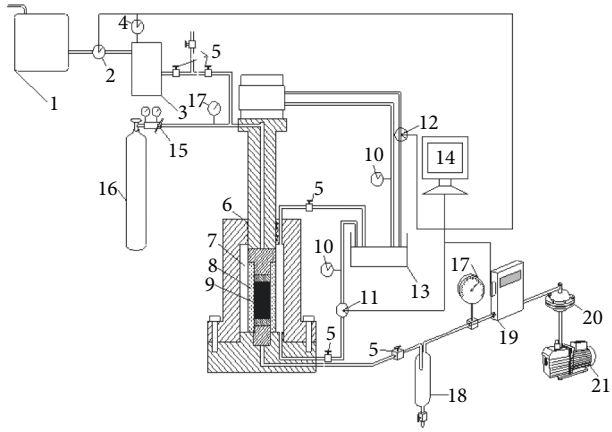

(a)

(b)

Figure 1: The system and physical figure of triaxial stress gas permeability simulation experiment device: (a) system figure and (b) physical figure. 1 – water tank, 2 – water flow meter, 3 – metering pump, 4 – water pressure gauge, 5 – the valve, 6 – O-ring seal, 7 – pressure chamber, 8 – confining pressure booster aprons, 9 – coal test specimen, 10 – oil pressure gauge, 11 – confining pressure control valve, 12 – axial pressure control valve, 13 – fuel tank, 14 – computer, 15 – pressure release valve, 16 – high pressure gas, 17 – gas pressure gauge, 18 – gas-water separator, 19 – the gas flow meter, 20 – damper, and 21 – vacuum pump.

4.2. Analysis of Experimental Results. According to the permeability datum, the permeability and effective stress evolution characteristic curves of coal samples P1, P2, V1, and V2 under the same loading and unloading path are shown in Figure 4.

(1) In the stress loading process, the gas permeability change trends of the coal samples are similar. The permeability decrease with increasing effective stress. The permeability of the P1 and P2 decrease by 84.95% and 84.92%, respectively, when the effective stress reaches 7.75 MPa; meanwhile, the permeability of the V1 and V2 coal samples decrease by 57.30% and 57.25%, respectively. When the effective stress reaches its maximum value of 11.75 MPa, the permeability of the four coal samples fall to 0.00156 mD, 0.00182 mD, 0.00432 mD, and 0.00494 mD, respectively, falling by 98.34%, 98.32%, 75.83%, and 75.97%. P1 and P2 almost lose their permeability capacity. This shows that the four coal

(a)

(b)

Figure 2: Processing and forming of coal samples: (a) machining forming drilling of coal samples and (b) polishing and forming of coal sample.

(a) (b)

Figure 3: Samples with different bedding fracture directions: (a) parallel bedding and (b) vertical bedding.

samples had a significant response to the loading stress in the initial stages of loading. The main reason for this is that cracks are prone to closure under compression, and the permeability decrement is initially rapid albeit it slowed later. The phenomenon could be explained that with the increase of effective stress, the coal sample undergoes three stages [18], namely, crack compaction, elastic deformation, and plastic deformation. When the effective stress is less than 9.75 MPa, the permeability changes rapidly, which can be judged as the coal sample experiencing the first two stages. When the effective stress is greater than 9.75 MPa, the coal samples enter the plastic deformation stage. The coal samples are gradually compacted, and the permeability become smaller and smaller, and the decrease of permeability gradually become stable, until their permeability were almost lost [19].

The initial gas permeability values of samples P1, P2, V1, and V2 are 0.09396 mD, 0.10814 mD, 0.01787 mD, and 0.02056 mD, respectively, and the ratios of the permeability value of samples with parallel bedding and samples with vertical bedding, namely, k_{0P1}/k_{0V1} and k_{0P2}/k_{0V2} were 5.258 and 5.260, respectively, which indicates that gas is more

Table 1: The experimental scheme.

	Inlet gas pressure, P_1 (MPa)	Outlet gas pressure, P_2 (MPa)	Axial compression, σ_z (MPa)	Confining pressure, σ_w (MPa)	Effective stress, σ_e (MPa)
Loading process	0.6	0.1	2	2	1.75
	0.6	0.1	4	4	3.75
	0.6	0.1	6	6	5.75
	0.6	0.1	8	8	7.75
	0.6	0.1	10	10	9.75
	0.6	0.1	12	12	11.75
Unloading process	0.6	0.1	12	12	11.75
	0.6	0.1	12	10	10.42
	0.6	0.1	12	8	9.08
	0.6	0.1	12	6	7.75
	0.6	0.1	12	4	6.42
	0.6	0.1	12	2	5.08

Table 2: Permeability of parallel bedding direction coal samples during the loading and unloading process.

	Effective stress, σ_e (MPa)	Permeability, k (mD)			Effective stress, σ_e (MPa)	Permeability, k (mD)	
		Coal sample, P1	Coal sample, P2			Coal sample, P1	Coal sample, P2
Loading process	1.75	0.09396	0.10814	Unloading process	11.75	0.00156	0.00182
	3.75	0.04329	0.04864		10.42	0.00192	0.00243
	5.75	0.02491	0.03096		9.08	0.00262	0.00314
	7.75	0.01414	0.01631		7.75	0.00363	0.00428
	9.75	0.00784	0.01002		6.42	0.00463	0.00528
	11.75	0.00156	0.00182		5.08	0.00511	0.00612

Table 3: Permeability of vertical bedding direction coal samples during the loading and unloading process.

	Effective stress, σ_e (MPa)	Permeability, k (mD)			Effective stress, σ_e (MPa)	Permeability, k (mD)	
		Coal sample, V1	Coal sample, V2			Coal sample, V1	Coal sample, V2
Loading process	1.75	0.01787	0.02056	Unloading process	11.75	0.00432	0.00494
	3.75	0.01226	0.01421		10.42	0.00514	0.00591
	5.75	0.00932	0.01072		9.08	0.00565	0.00651
	7.75	0.00763	0.00879		7.75	0.00635	0.00732
	9.75	0.00594	0.00684		6.42	0.00737	0.00841
	11.75	0.00432	0.00494		5.08	0.00866	0.00991

likely to flow along the bedding direction [20]. As seen in Figure 5, the permeability of coal samples P1 and P2 are almost bigger than that of V1 and V2. When the effective stress reaches 11.75 MPa, the permeability of P1 and P2 coal samples become smaller than that of V1 and V2. It can be predicted that with the further increase of stress, the permeability of the parallel bedding coal sample would approach 0.

The relations between permeability and effective stress in the loading process of the four coal samples are obtained through the exponential fitting of permeability evolution characteristics. The relationship between permeability and effective stress is $k = ye^{x\sigma_e}$ (where k is the permeability, σ_e is effective stress, x and y are the fitting coefficients, and R^2 is the correlation coefficient), and the fitting results are shown in Table 4. The fitting coefficients x of coal samples P1 and P2 (−0.3745 and −0.3686) are much smaller than that of V1 and V2 (−0.1353 and −0.1364), which also fully indicate that the permeability decrease amplitude of parallel bedding is larger than that of vertical bedding.

(2) In the stress unloading process. the permeability of the four coal samples increases with decreasing of effective stress, and the increasing trend of permeability is consistent. However, the increasing amplitude is somewhat different. The permeability of the four coal samples (P1, P2, V1, and V2) recover to 168%, 173%, 131%, and 132% of the minimum value, respectively, when the effective stress falls from 11.75 to 9.08 MPa. The permeability increments are 328%, 336%, 200%, and 201% when the effective stress is 5.08 MPa.

In the unloading process, each coal sample has a permeability value corresponding to certain effective stress (11.75 MPa, 1.42 MPa, 9.08 MPa, 7.75 MPa, 6.42 MPa, and 5.08 MPa). The permeability under the same effective stress in the loading process could be calculated through the fitting

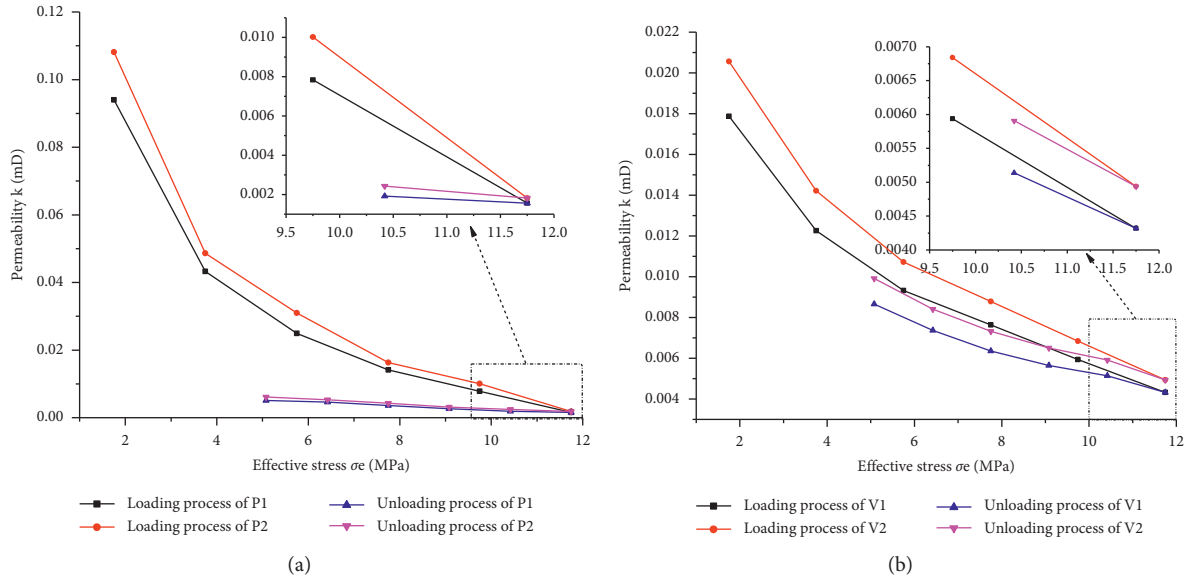

Figure 4: Permeability evolution characteristics of coal samples during the loading and unloading process. (a) parallel bedding and (b) vertical bedding.

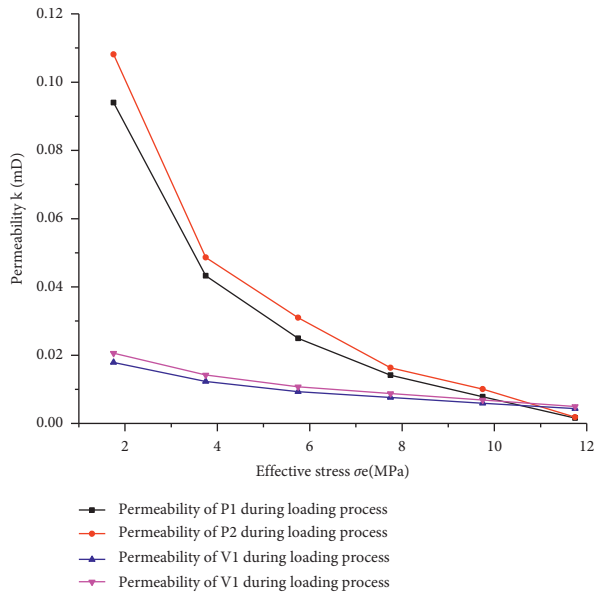

Figure 5: Characteristic curve of permeability evolution with effective stress during the stress loading process.

Table 4: Fitting results about the relationship between permeability and effective stress during the loading process.

Coal samples	y	x	R^2
P1	0.2013	−0.3740	0.954
P2	0.2299	−0.3686	0.944
V1	0.0214	−0.1353	0.992
V2	0.0247	−0.1364	0.992

formulas corresponding to the coal sample during the loading process (the fitting formulas of the four coal samples were shown in Table 4), and the calculation results are shown in Table 5.

In the unloading process, the permeability of coal samples could not be fully restored to the value of the same effective stress corresponding to the loading process. In other words, under the same effective stress, there is a certain difference in the permeability of coal samples during the loading and unloading process. This difference reflects the loss of permeability. The larger the loss, the lower the degree

Table 5: Calculated permeability value and actual permeability value at the same effective stress.

Effective stress	Calculated permeability value in the loading process				Actual permeability value in the unloading process			
	P1	P2	V1	V2	P1	P2	V1	V2
11.75	0.00249	0.00302	0.00436	0.00500	0.00156	0.00182	0.00432	0.00494
10.42	0.00409	0.00494	0.00523	0.00599	0.00192	0.00243	0.00514	0.00591
9.08	0.00675	0.00809	0.00626	0.00718	0.00262	0.00314	0.00565	0.00651
7.75	0.01109	0.01321	0.00750	0.00861	0.00363	0.00428	0.00635	0.00732
6.42	0.01824	0.02157	0.00898	0.01032	0.00463	0.00528	0.00737	0.00841
5.08	0.03011	0.03534	0.01076	0.01238	0.00511	0.00612	0.00866	0.00991

of permeability recovery, and the higher the anti-sense permeability recovery. The ratio between permeability loss and seepage rate in the loading process could be defined as permeability loss damage rate [21, 22].

The loss rate of coal sample permeability could be used to evaluate the decreased range of coal sample permeability. The higher the damage rate of coal samples permeability, the greater the decrease range of coal samples permeability. The damage rate of coal sample permeability could be calculated according to the following formula [23, 24]:

$$D = \frac{(k_c - k_a)}{k_c} \times 100, \tag{3}$$

where D is the damage rate of coal sample permeability, k_a is the actual permeability value in the unloading process, and k_c is the calculated permeability value in the loading process by the relevant fitting formula. The permeability loss rate of coal sample under the same effective stress is shown in Table 6. The curve of permeability loss rate and effective stress can be drawn according to Table 6, as shown in Figure 6.

As can be seen from Figure 6, the permeability loss rates of the four coal samples increase with the decrease of the effective stress. When the effective stress decrease to 5.08 MPa, the loss rates of the coal sample P1 and P2 are as high as 80%, while the loss rates of the coal sample V1 and V2 are less than 20%. These indicate that the degree of fracture compaction of the parallel bedding coal samples after compression is much higher than that of the vertical bedding coal samples. Even after stress unloading, the degree of fracture recovery is low.

In the process of stress unloading, the change characteristics of permeability with effective stress of the four coal samples are shown in Figure 7. It can be seen that the permeability of the parallel bedding coal samples are always lower than that of the vertical bedding coal samples during the whole unloading process.

(3) The unloading process of coal samples is not a simple inverse process of the loading process, which can be explained by the deformation of coal sample during stress loading and unloading, as shown in Figure 8.

The permeability continues to recover with the unloading of effective stress, but the recovery degree of a different coal sample is significantly different. When the maximum loading stress of the coal sample is less than the elastic limitation (A) in the loading stage, there is no plastic damage in the sample, which belongs to the category of elastic deformation. The pores and cracks in the sample can completely be restored after the stress is removed. On the contrary, the stress-strain curve will deviate from the curve of the loading process and are unable to return to the origin, as the PC curve shown in Figure 8.

Table 6: Permeability loss rate of coal sample under the same effective stress.

Effective stress	DP1 (%)	DP2 (%)	DV1 (%)	DV2 (%)
11.75	37.22	39.82	1.03	1.14
10.42	53.02	50.78	1.64	1.30
9.08	61.16	61.19	9.81	9.39
7.75	67.28	67.60	15.30	14.97
6.42	74.62	75.52	17.91	18.48
5.08	83.03	82.68	19.54	19.94

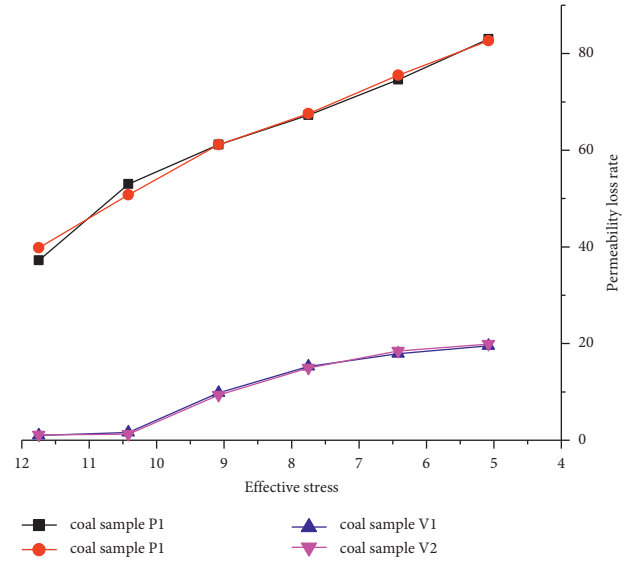

Figure 6: Curve of permeability loss rate and effective stress.

5. Engineering Verification

The test mine is a coal and gas outburst mine. The average thickness of No. 3 coal seam is 6 m; the bedding fissure is developed along the dip direction coal seam; and the gas content of the coal seam reaches 12 m^3/t on average, having the characteristics of large outburst risk, low coal seam permeability coefficient, and poor degas effect. According to the "Rules for Prevention and Control of Coal and Gas Outbursts" in China (revised in 2019), two ways of gas predrainage are taken to protect the coal roadway tunneling, including drilling boreholes through the floor rock roadway and along the coal seam [25].

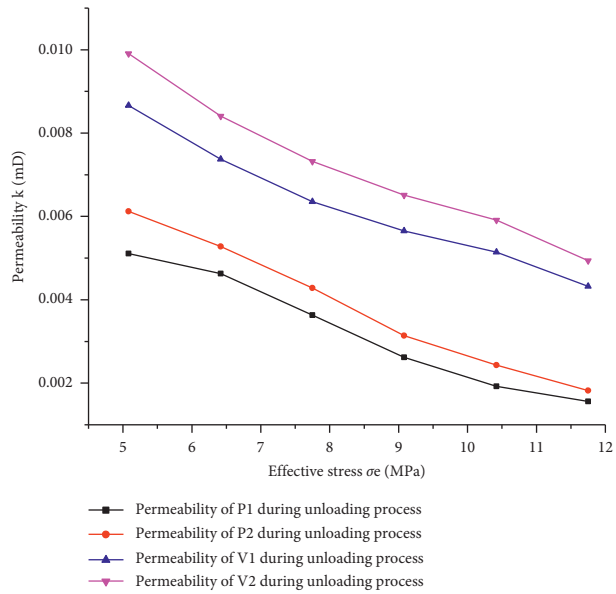

Figure 7: Characteristic curve of permeability evolution with effective stress during the stress unloading process.

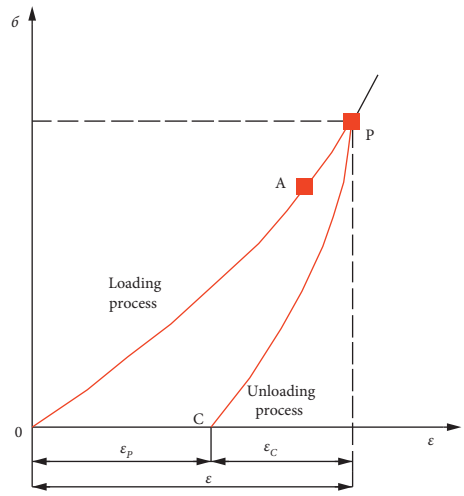

Figure 8: Stress-strain curve of coal sample during loading and unloading.

The return air roadway of 11,053 working face has been tunneled through. Before heading into the intake airway of 11,053 working face, drilling boreholes along coal seams in the direction of the intake airway are arranged in the return air roadway; meanwhile, drilling boreholes through coal seams are arranged in the floor rock roadway, as shown in Figure 9.

Arrangement of the two types of drilling is approximately perpendicular and parallel to the direction of bedding, respectively, being regarded as parallel bedding and vertical bedding gas drainage boreholes. With the advance of the driving working face, there will be three zones of stress in front of the working face, namely, pressure relief zone, stress concentration zone, and original stress zone [26]. A group of parallel bedding and vertical bedding gas drainage boreholes were selected to monitor the gas drainage concentration for 40 days. At this time, the gas drainage concentration of the two groups reflects the permeability of gas along the direction of coal bedding and vertical bedding during stress loading and unloading. The gas drainage concentration of the two groups of boreholes is shown in Table 7. Curves about gas drainage concentration with time of parallel and vertical bedding drilling boreholes are drawn according to the monitored datum, as shown in Figure 10.

According to Figure 10, it can be seen that in the early stage of gas concentration monitoring, the gas drainage concentration of the two groups of drainage holes did not change much, mainly because the in situ stress conditions of the drilling holes did not change, and they were both in the original stress zone. However, the gas concentration of the vertical bedding gas drainage boreholes was always greater than that of the parallel bedding boreholes (sections P_a–P_b and V_a–V_b in Figure 10).

As the roadway moved forward, the stress concentration zone also moved forward, and the stress at the location of the gas drainage hole increased, which was equivalent to loading the coal body [27]. With the increase of loading stress, the permeability of the coal body at the drilling hole became lower and lower, and the gas drainage concentration of the drilling hole also decreased. When the stress was loaded to the peak value, the permeability of the coal seam dropped to the lowest value in the loading process, which reflected that the gas drainage concentration was the lowest (sections P_b–P_c and V_b–V_b in Figure 10). This stage was equivalent to the stress loading stage in the experimental process. It could be seen that the permeability in the vertical bedding direction of the coal body is always greater than that in the parallel bedding direction during the whole loading process.

With the further advance of the tunneling roadway, the stress concentration zone continued to advance, and the stress on the coal body became smaller and smaller [28, 29]. The permeability of coal increased with the stress unloading; the reaction to the gas drainage holes was that the gas drainage concentration was getting higher and higher

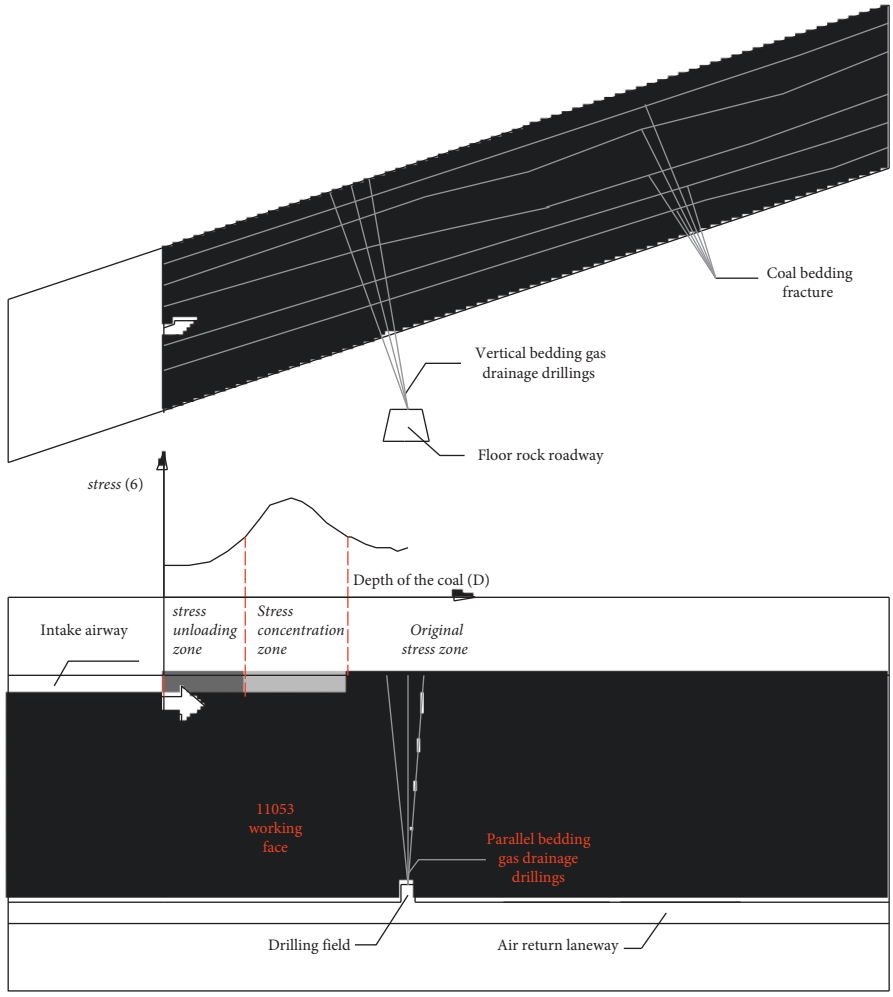

Figure 9: Gas drainage drillings layout along and through layers layout in 11,053 working face.

Table 7: Gas concentration of parallel bedding and vertical bedding drilling boreholes.

Ged (d)	Gc (%)		Ged (d)	Gc (%)		Ged (d)	Gc (%)		Ged (d)	Gc (%)	
	Pd	Vd		Pd	Vd		Pd	Vd		Pd	Vd
1	39.43	53.22	21	5.81	7.47	11	36.94	49.86	31	53.12	75.95
2	39.84	53.78	22	12.45	17.43	12	34.03	45.94	32	59.35	82.59
3	39.01	52.66	23	17.43	24.07	13	31.54	42.58	33	64.74	87.64
4	40.26	54.34	24	23.66	31.96	14	28.22	38.1	34	68.89	84.23
5	40.67	54.9	25	28.22	38.6	15	24.9	33.62	35	67.65	86.71
6	39.84	53.78	26	31.96	45.65	16	22.41	30.25	36	68.89	87.11
7	40.26	54.34	27	35.28	51.88	17	19.51	26.33	37	67.65	85.12
8	41.09	55.46	28	39.01	57.69	18	16.19	21.85	38	67.23	87.63
9	39.84	53.78	29	43.58	63.08	19	11.21	15.13	39	68.06	85.42
10	39.01	52.66	30	46.9	68.48	20	6.23	8.4	40	68.89	83.45

Notes. Ged – gas extraction days, Gc – gas concentration, Pd – parallel bedding drilling, and Vd – vertical bedding drilling.

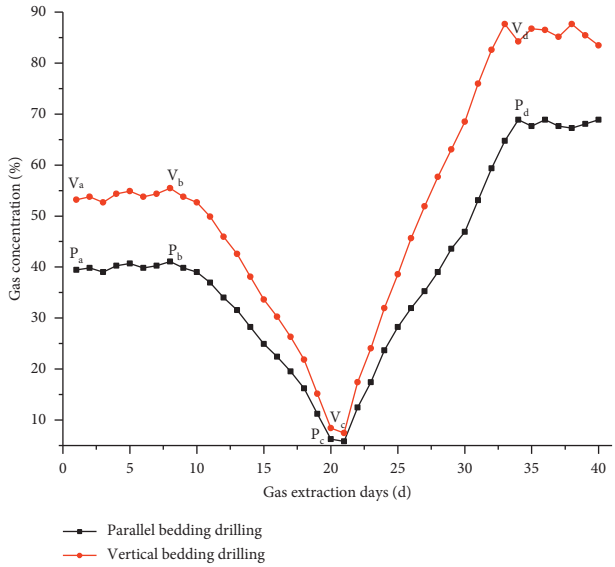

Figure 10: Curve about gas drainage concentration with time of parallel and vertical bedding drilling boreholes.

(sections P_c–P_d and V_c–V_d in Figure 10). This stage was equivalent to the stress unloading stage in the experimental process. In the whole unloading process, the permeability in the vertical bedding direction of the coal body was also always greater than that in the parallel bedding direction.

6. Conclusion

(1) In the stress loading process, the permeability of the parallel bedding coal sample would approach 0. Therefore, gas drainage boreholes should not be arranged in a direction along the bedding in the severely compressed seam.

(2) In the stress unloading process, it could be seen that the permeability of the parallel bedding coal samples are always lower than that of the vertical bedding coal samples during the whole unloading process. Therefore, in the stress-relieved coal seam, gas drainage boreholes should be arranged vertically to the bedding fissure to maximise the gas drainage effect.

(3) Field engineering practice also proves that when gas drainage is arranged in the coal seam containing bedding cracks, the drilling direction should be perpendicular to the bedding direction as far as possible, so as to improve the gas drainage effect.

The results of laboratory study and engineering practice provide some guidance for the rational arrangement of gas drainage boreholes and improvement of gas drainage concentration in the coal mine. This ensures the sustainability of the gas drainage effect and is of great significance to reduce the occurrence of mine gas accidents.

Data Availability

The data used to support the findings of this study are included within the article.

Conflicts of Interest

The authors declare that they have no conflicts of interest.

Acknowledgments

The authors gratefully acknowledge the financial support from the National Natural Science Foundation of China (52174168), the Science and Technology Innovation Team Program of Henan Universities (22IRTSTHN009), the Science and Technology Project of Henan Province for Tackling Key Problems (222102320466), the Research and Cultivation Fund of Henan University of Engineering (PYXM202017), and the Research Project of Education and Teaching Reform of Henan University of Engineering (2021JYYB001).

References

[1] J. Liu, H. Sun, L. Yi, and C. Jie, "Current situation and development trend of coalbed methane development and utilization technology in coal mine area," *Journal of China Coal Society*, vol. 45, no. 1, p. 258, 2020.

[2] X. Chen, R. Liu, and B. Xie, "Productivity model of fractured horizontal wells in shale oil reservoirs with bedding fractures considered," *Xinjiang Oil & Gas*, vol. 18, no. 1, pp. 73–79, 2022.

[3] F. Zhang, "Gas technology of uniform pressure sealing gas drainage in fissure development area," *Safety In Coal Mines*, vol. 51, no. 3, pp. 79–83, 2020.

[4] W. Zhang, C. Zheng, S. Xue et al., "Study on gas drainage characteristics based on permeability anisotropy of coal," *Safety in Coal Mines*, vol. 51, no. 7, pp. 6–11, 2020.

[5] G. Yue, H. Liu, J. Yue, and M. W. Li, "Influence radius of gas extraction borehole in an anisotropic coal seam: underground in-situ measurement and modeling," *Energy Science & Engineering*, vol. 7, no. 3, pp. 694–709, 2019.

[6] X. Huang, "Experimental study on influence of structural anisotropy of coal upon gas permeability," *Mining Safety and Environmen-tal Protection*, vol. 39, no. 2, pp. 1–3, 2012.

[7] R. Pan, Y. Cheng, and J. Dong, "Research on permeability characteristics of layered natural coal under different loading and unloading," *Journal of China Coal Society*, vol. 39, no. 3, pp. 473–477, 2014.

[8] B. Deng, X. Kang, and L. I. Xing, "Effect of different bedding directions on coal deformation and permeability characteristic," *Journal of the China Coal Society*, vol. 40, no. 4, pp. 888–894, 2015.

[9] P. Cen, K. Tian, E. Wei, S. Liu, and C. Bi, "Axial effect of gas seepage in bedding fractured coal under multistage loading and unloading and its application," *Safety In Coal Mines*, vol. 52, no. 12, pp. 9–14, 2021.

[10] S. Wang, D. Elsworth, and J. Liu, "Permeability evolution in fractured coal: the roles of fracture geometry and water-content," *International Journal of Coal Geology*, vol. 87, no. 1, pp. 13–25, 2011.

[11] Y. Wu, J. Liu, D. Elsworth, and H. X. Siriwardane, "Evolution of coal permeability: c," *International Journal of Coal Geology*, vol. 88, no. 2-3, pp. 152–162, 2011.

[12] H. Li, S. Shimada, and M. Zhang, "Anisotropy of gas permeability associated with cleat pattern in a coal seam of the Kushiro coalfield in Japan," *Environmental Geology*, vol. 47, no. 1, pp. 45–50, 2004.

[13] D. Yu, Z. Yang, Y. Guo, Y. G Yang, and B Wang, "Inversion method of initial geostress in coal mine field based on FLAC^{3D} transverse isotropic model," *Journal of China Coal Society*, vol. 45, no. 10, pp. 3427–3434, 2020.

[14] K. Tian and G. Wang, "Gas seepage behaviors revealed by two kinds of typical soft and hard raw coals under high pressure water," *International Journal of Earth Sciences and Engineering*, vol. 9, no. 2, pp. 866–871, 2016.

[15] J. Wei, D. Wang, and W. E. I. Le, "Comparison of permeability between two kinds of loaded coal containing gas samples," *Journal of China Coal Society*, vol. 38, no. Supp. 1, pp. 93–99, 2013.

[16] X. Yuan, B. Liang, and W. Sun, "Research on permeability evolution model for coal seam being drained by pressure relief," *China Safety Science Journal*, vol. 26, no. 2, pp. 127–131, 2016.

[17] A. L. A. M. A. K. M. Badrul, N. Masaki, Y. O. S. H. I. A. K. I. Fujii, F Daisuke, and K Jun-ichi, "Effects of confining pressure on the permeability of three rock types under compression," *International Journal of Rock Mechanics and Mining Sciences*, vol. 65, pp. 49–61, 2014.

[18] J. Liu, *Seepage Characteristics of Loaded Coal under True Triaxial and Its Application in Gas Extraction*, China University of Mining and Technology, Beijing, China, 2017.

[19] R. Pan, *The Permeability Evolution Characteristics of Loaded Coal and Its Application in the Drainage of Pressure-Relief Gas*, China University of Mining and Technology, 2014.

[20] H. Yu, F. Chen, W. Chen, J. Yang, J. Cao, and K. Yuan, "Research on permeability of fractured rock," *Chinese Journal of Rock Mechanics and Engineering*, vol. 31, no. S1, pp. 2788–2795, 2012.

[21] M. Thommes, K. Kaneko, and A. V. J. P. F. J. K. S. W Neimark, "Physisorption of gases, with special reference to the evaluation of surface area and pore size distribution (IUPAC Technical Report)," *Pure and Applied Chemistry*, vol. 87, no. 9-10, pp. 1051–1069, 2015.

[22] Y. Liu, "Experimental analysis of coal permeability evolution under cyclic loading[J]," *Journal of China Coal Society*, vol. 44, no. 8, pp. 2579–2588, 2019.

[23] D. Wang, J. Wei, and G. Yin, "Investigation ON change rule OF permeability OF coal containing gas under complex stress paths," *Chinese Journal of Rock Mechanics and Engineering*, vol. 31, no. 2, pp. 303–310, 2012.

[24] M. Jing and X. Yuan, "Experimental research ON core stress sensitivity OF carbonate rock," *Natural Gas Industry*, vol. 20, no. S, pp. 114–117, 2002.

[25] State Administration of Coal Mine Safety, *Rules for Prevention and Control of Coal and Gas Outbursts*, Coal Industry Press, 2019.

[26] J. Gao and S. Hou, "Dynamic distribution of gas pressure and emission Around adiving roadway," *Journal of China Coal Society*, vol. 32, no. 11, pp. 1127–1131, 2007.

[27] F. Cai and Z. Liu, "Simulation and experimental research on upward cross-seams hydraulic fracturing in deep and low-permeability coal seam," *Journal of China Coal Society*, vol. 41, no. 1, pp. 113–119, 2016.

[28] X. Kong, E. Wang, Q. Liu, and Z. D. Z. Y. Li, "Dynamic permeability and porosity evolution of coal seam rich in CBM based on the flow-solid coupling theory," *Journal of Natural Gas Science and Engineering*, vol. 40, pp. 61–71, 2017.

[29] J. Fu, X. Fu, and Y. Jiang, "Fundamental study on gas drainage and extraction from pressure-relieved zone of a single seam with low gas permeability," *Mining Safety & Environmental Protection*, vol. 39, no. 1, pp. 4–7, 2012.